OPEN

PRS GLOBAL OPEN

ORIGINAL ARTICLE

Pediatric/Craniofacial

Metallic Fixation of Mandibular Segmental Defects: Graft Immobilization and Orofacial Functional Maintenance

Narges Shayesteh Moghaddam, MSc*
Ahmadreza Jahadakbar, MSc*
Amirhesam Amerinatanzi, MSc*
Mohammad Elahinia, PhD*
Michael Miller, MD†
David Dean, PhD†

Background: The aim of this study is to investigate the behavior of the healthy mandible under maximum molar bite force to demonstrate the problems associated with the current standard of care procedures for mandibular segmental defect reconstruction (ie, use of Ti–6Al–4V hardware and either a single- or double-barrel fibular graft). With current Ti–6Al–4V mandibular reconstruction hardware, there is a significant stiffness mismatch among the hardware, graft, and the remaining host anatomy. How the distribution of mechanical forces through the mandible is altered after a segmental bone loss and reconstruction is incompletely understood.
Methods: We studied a healthy adult mandible for stress, strain, and reaction force distribution during normal mastication. Stress distribution of this model was then used to study problems encountered after mandibular segmental defect reconstructive surgery. We model the use of both single- and double-barrel fibular grafts to repair the loss of the left $M_{1–3}$ containing segment of the mandible. These simulations were done using 2 sets of plates with different thicknesses.
Results: We found that the stiffness mismatching between the fixation hardware and the graft and host bone causes stress shielding of that bone and stress concentrations in the fixation hardware and screws. These effects are expected, especially during the bone healing period. However, long term, this abnormal stress–strain distribution may lead to either the hardware's failure due to stress concentration or graft failure due to bone resorption as a result of stress shielding. We found that the stress–strain distribution is more normal with a double-barrel fibular graft. Additionally, we found that thinner fixation plates can reduce stress shielding.
Conclusion: The proposed model can be used to evaluate the performance and optimization of the fixation device. *(Plast Reconstr Surg Glob Open 2016;4:e858; doi: 10.1097/GOX.0000000000000859; Published online 8 September 2016.)*

Mandibular segmental defects are defined as a loss of mandibular bone that results in a complete gap. This gap is considered a "critical size" defect if it cannot be healed without an intervention.[1] These defects are usually caused by surgical resection of tumors, trauma, infection, or radiation-induced tissue damage associated with cancer treatment (osteoradionecrosis).[2]

*From the *Department of Mechanical Industrial and Manufacturing Engineering, University of Toledo, Toledo, OH; and †Department of Plastic Surgery, The Ohio State University, Columbus, OH.*

Received for publication December 30, 2015; accepted June 17, 2016.

DOI: 10.1097/GOX.0000000000000859

The purpose of mandibular reconstruction is to restore normal appearance, mastication, speech, swallowing, and breathing.[3,4] The most reliable means of restoring critical size or larger mandibular segmental defects is the use of a vascularized bone transfer, usually harvested from the fibula or iliac crest.[3,5] Typically, 1 or more surgical grade 5 (Ti–6Al–4V)[6,7] fixation devices are used to immobilize the graft.[8–11] Ti–6Al–4V is the most common Ti alloy because it offers unique characteristics including biocompatibility, formability, high strength, light weight, and wear resistance.[6] Because this hardware is often left in place after the bone has healed, it may subsequently cause stress

Disclosure: *The authors have no financial interest to declare in relation to the content of this article. This study was supported by Ohio Third Frontier Technology Validation and Startup Fund (TVSF) grant 15-791. The Article Processing Charge was paid for by the Department of Plastic Surgery, The Ohio State University (Columbus, OH).*

shielding or stress concentrations, due to its high stiffness compared with the surrounding host bone.[7] The former may result in resorption of the shielded bone,[12] and the latter may result in hardware failure.[13]

Segmental defects of the mandible occur in different lengths. Smaller defects (eg, <6 cm) with healthy adjacent soft tissue can often be restored using a bone graft harvested from the iliac crest. A large amount of bone can be harvested from the iliac crest. Iliac crest grafts can provide sufficient bone to allow dental restoration using osseointegrated implants.[5,12] Larger defects with poor quality soft tissue require a vascularized bone graft. In this procedure, the bone is transferred along with a vascular pedicle that requires microsurgery to connect the vascular pedicle to blood vessels near the defect. The fibula is a common site for the harvest of a vascularized bone graft. It provides a long bone segment, a reliable (ie, easily found) vascular pedicle with large diameter vessels and its removal causes minimal donor site morbidity.[3,5,14,15] The fibula also permits cutting and folding the bone segments together to create a "double barrel" of bone that is stronger and has roughly double the height of a single-barrel fibular graft.[10,16] This procedure offers several advantages. It provides more vertical height, which improves the stability of dental implants.[17] The reduced height of a single-barrel fibular graft provides less depth for dental implant posts and results in more torque on the exposed portion of the dental implant post as it extends between the top of the graft to the occlusal plane.[18] This unfilled gap may also cause a loss of facial contour.[16,19,20]

It should be noted that the maximum width of a defect which can be filled by a double-barrel fibular graft taken from one calf is 10 cm. This limitation is due to the maximum fibular length, which is 24 cm. Along with its vascular pedicle and overlying skin flap, this graft is often halved in length while preserving the blood supply. Next, the 2 segments are folded on top of each other.[16] The harvesting of a segment that is too long may increase the risk of donor site morbidity[17] and/or knee or ankle joint instability.[21]

Mandibular reconstruction with a double-barrel fibular graft requires additional fixation devices to attach the upper barrel to the superior border of the remaining host mandible.[16–19] Often mini-plates are used to attach the upper barrel as they provide sufficient stability and reduce the surgical time and discomfort for patients.[22–24]

To study the failure risk of the reconstruction surgery, stress distribution is a good criterion.[25–27] By comparing the stress distribution on the reconstructed mandible, we can detect the potential regions of failure and propose solutions. How the distribution of mechanical forces through the mandible is altered after segmental bone loss and reconstruction is incompletely understood? A better understanding may facilitate optimizing reconstruction so as to restore the normal mechanical properties of the entire mandible. We begin our study by investigating the biomechanical behavior (ie, stress,[28] strain,[28] and reaction forces[29,30]) of a complete, normal mandible with a finite element (FE) model that discriminates cortical and cancellous bone, muscle, periodontal ligament, and the teeth. The objectives of our study are to investigate and contrast stress distribution at similar areas of the mandible for 3 cases of mastication at M_1: (1) a healthy mandible under normal chewing conditions, (2) a resected mandible (ie, segmental defect in the M_{1-3} region) with a single-barrel fibular graft and Ti–6Al–4V fixation hardware, and (3) a resected mandible with a double-barrel fibular graft and Ti–6Al–4V fixation hardware. For each case of reconstruction, 2 sets of plates with different thicknesses are used to study the effect of thickness on the fixation plates.

MATERIALS AND METHODS

Computed Tomography Scans and Design of Three-dimensional Mandible Models

A computer-aided model of a normal mandible (ie, healthy adult female, approximately 25–30 y of age) was created from computed tomography scan data. Separate computed tomography data are fit to these surfaces to locate the periodontal ligament and the fibular graft.[31,32] The resected area of the mandible includes the left segment bearing M_{1-3}, which has a length of 40 mm. Components of the reconstruction, including the fibular graft, the metallic fixation plates, and screws, are all simulated in SolidWorks (Dassault Systèmes, Waltham, MA). The fixation plate holding the inferior fibular barrel graft has 9 threaded holes, a thickness of 1.5 mm, length of 78 mm, and a width of 4 mm.[22] We graphically bent this plate to match the shape of the buccal (external) surface of the grafted bone and the adjacent host mandibular anatomy (ie, the inferior border of the mandible). We verified the fixation bar's contact with the bone surface by a collision detection algorithm. (Note: These plates are usually bent in the Operating Room and their close contact with the underlying bone is verified manually. The residual stress[33] on these plates would be negligible because the amount of bending is low.) For each fixation device, a minimum of 1 screw is placed in each of the remaining mandible segments and 1 screw on the opposing side of the fibular barrel graft (ie, screws are placed on both sides of the host bone/graft gap). Bicortical screws (ie, screws that pass through both the lingual and buccal cortices of the graft and the remaining host mandible) are used to fasten the large inferior plate.[22] The simulated screws have a diameter of 1.4 mm. The single-barrel fibular graft consists of cortical and cancellous bone layers with a height of 20 mm and a width of 14 mm. The vascularized, double-barrel fibular graft consists of 2 single-barrel grafts, fixed together by the surgeon to best mimic the normal contour of the mandible.[22] The height of the 2 adjacent pieces of the double-barrel graft is 38 mm.[17] To fixate the upper (second) fibular barrel graft, we simulate 2 mini-plates, both of which are slightly bent to fit tightly onto the graft and the superior border of the remaining host mandible. Each mini-plate has 3 threaded holes and is 1 mm thick with a length of 18 mm and a width of 2.8 mm. The mini-plates are secured by unicortical screws.[7,22] The diameter of the 4 screws securing each mini-plate is 1.4 mm. To study the effect of thickness of the fixation plates, another set of plates with an increased thickness (2.5 mm for the fixation plate holding the inferior fibular barrel graft

and 1.5 mm for the mini-plates) was designed and prepared for the simulations. It should be noted that all screws are locked into the plate and into the bone. All of the components were imported into ABAQUS[34] software (Dassault Systèmes, Waltham, MA) to conduct an FE analysis[35] of the expected stress—strain trajectories during mastication at the right M_1.

A 4-node linear tetrahedral mesh[34] was used for all 3 aforementioned cases of mastication. Based on mesh convergence analysis, the numbers of elements are 1512877, 1400426, and 1545228 for the normal mandible, a mandible reconstructed using Ti–6Al–4V hardware and a single-barrel fibular graft, and a mandibular reconstruction using Ti–6Al–4V hardware and a double-barrel fibular graft, respectively. All data pertaining to material properties[25] of our model components are taken from studies by Andani et al,[36] Shetty et al,[37] and Nagasao et al[38] as summarized in Table 1.

Constraints and Loading

We set up 24 nodes on the outer cortical surface of both mandibular condyles. This allows them to be restrained from movement in all 3 directions.[29] Seven nodes of bite contact on the buccal cusps of the lower right first molar are constrained from movement in all directions, simulating peak bite force (ie, these cusps reach maximal approximation between the buccal and lingual cusp rows of the upper molars).[22,29] The intersections between teeth/periodontal ligament and periodontal ligament/mandible are tied together completely and homogenously; there is no gap initially between the grafted bone and the remaining host mandible. The fixation hardware holds these 2 surfaces closely together.[29] Table 2 shows all of the muscle forces and directions, and also the area of each muscle attachment. Muscle forces are distributed homogeneously across the area of attachment in all muscles. The values for the area of attachment are taken from Van Eijden et al.[39] Muscle forces after mandibular reconstruction are assumed to be 60% of the average value recorded for a healthy adult.[22] Following reconstruction, all of the muscles are restored to their normal location. This meant that in some cases small amounts of the muscular sleeve would overlie the grafted bone and the remaining host mandible (Table 2).

Model Validation

To validate our model, the experimental data were obtained from a study given by Ichim et al.[40] The scope of their study was to measure the buccal and lingual strains under normal loading conditions using a dry mandible. The boundary and loading conditions were subsequently recreated in our FE model.[41] To derive the strain based on our FE results, the $\Delta 1/1$ values for the similar regions to the experimental model were calculated (Fig. 1).

As shown in Figure 1, the results show a very good agreement between the model-predicted strains and experimental strains. The correlations between the results are statistically significant (buccal side: $r > 0.99$, $P < 0.0005$, root mean square error < 2.8e–6; lingual side: $r > 0.99$, $P < 0.0005$, root mean square error < 6.42e–6). All FE-predicted results were within the range of 95% confidence interval of average experimental measurements.

RESULTS

Reaction Forces

As mentioned in the Materials and Methods section, all the muscle forces used in the simulations are based on the bite force of 526 N on the right first molar, extracted from Korioth et al.[29] The first step to study these results is to calculate the equivalent bite force based on the simulations and to compare with the reference. All the material properties, boundary conditions, and muscle forces of our model are the same as in the study by Korioth et al.[29]

Our simulation results found a bite force of 507.4 N, which is obtained from a summation of the nodes reaction force at the first lower right molar tooth during centric occlusion. This represents a 3% discrepancy with the experimental bite force (ie, 526 N) seen by Korioth et al.[29] This discrepancy may be due to differences in mandibular shape, our inclusion of the periodontal ligament, and minor differences in the muscle attachment sites. This agreement between the simulation and the experiment results verifies the accuracy and validity of our FE model.

Normal Mandibular Masticatory Loading

Figure 2 presents the von Mises stress[42] that occurs during mastication at the right M_1 in the normal adult mandible. The maximum peak stress regions occur on the right first molar tooth (17.6 MPa), the mandibular coronoid process on the balancing side (4.12 MPa), the buccal alveolar ridge of the cortical mandible in the right molar area (3.92 MPa), and at the mandibular neck of the condylar process on the balancing side (4.82 MPa). It should be noted that the maximum stress on the periodontal ligament is 1.4 MPa (Fig. 2).

Table 1. Material Properties of FE Model

	E_X	E_Y	E_Z	ν_{XY}	ν_{YZ}	ν_{XZ}	G_{XY}	G_{YZ}	G_{XZ}
Cortical									
Symphysis regions	23,000.0	15,000.0	10,000.0	0.3	0.3	0.3	6200	3600	4800
Angle regions	20,000.0	12,000.0	11,000.0	0.3	0.3	0.3	6000	5300	4800
Rest of mandible	17,000.0	8200.0	6900.0	0.315	0.325	0.31	4600	2900	2800
Cancellous bone	960.0	390.0	320.0	0.3	0.3	0.3	170	130	90
Teeth	17,600.0	17,600.0	17,600.0	0.25	0.25	0.25			
Periodontal ligament	2.7	2.7	2.7	0.45	0.45	0.45			

The terms E (Pa), G (Pa), and **ν** stand for modulus of elasticity,[25] modulus of rigidity,[25] and Poission's ratio[25] of the material, respectively.[36–38]

Table 2. Masticatory Muscle Vectors

Muscle Group	Working Side	Balancing Side
Masseter		
Superficial	−0.32i + 1.37j + 0.65k	+0.27i + 1.14j + 0.54k
Deep	−0.81i + 1.12j − 0.53k	+0.67i + 0.93j − 0.44k
Medial pterygoid	+1.09i + 1.76j + 0.82k	−0.78i + 1.26j + 0.59k
Temporalis		
Anterior	−0.19i + 1.27j + 0.05k	+0.15i + 1.01j + 0.04k
Middle	−1.07i + 4.08j − 2.43k	+1.08i + 4.14j − 2.46k
Posterior	−0.72i + 1.61j − 2.95k	+0.48i + 1.07j − 1.95k

The muscle forces shown here were distributed homogeneously across the area of attachment in our mastication FE model. i, j, and k are the same as the x, y, and z directions of the volume in which the FE analysis occurs. These directions are weighted within the equation for each muscle to determine the primary vector, the overall vector, toward which each of these muscles pulls on the mandible.[22,29,39]

Effect of Using Ti–6Al–4V Fixation Hardware and a Fibular Graft on Masticatory Stress Distribution

We graphically illustrate the change in stress at peak exertion during the chewing stroke for the case of a normal adult mandible, a resected mandible with a single-barrel fibular graft and Ti–6Al–4V fixation hardware, and a resected mandible with a double-barrel fibular graft and Ti–6Al–4V fixation hardware (Fig. 3). We see abnormal stress distribution in the mandible as a result of the Ti–6Al–4V fixation plate that is attached to either a single-barrel fibular graft or a double-barrel fibular graft. This analysis leads to 2 concerns for patients where the fixation hardware is not removed after the grafted fibular bone has healed with the remaining host mandible: (1) stress shielding of some of the grafted bone and host mandible and (2) stress concentration, especially at the fixation screws.

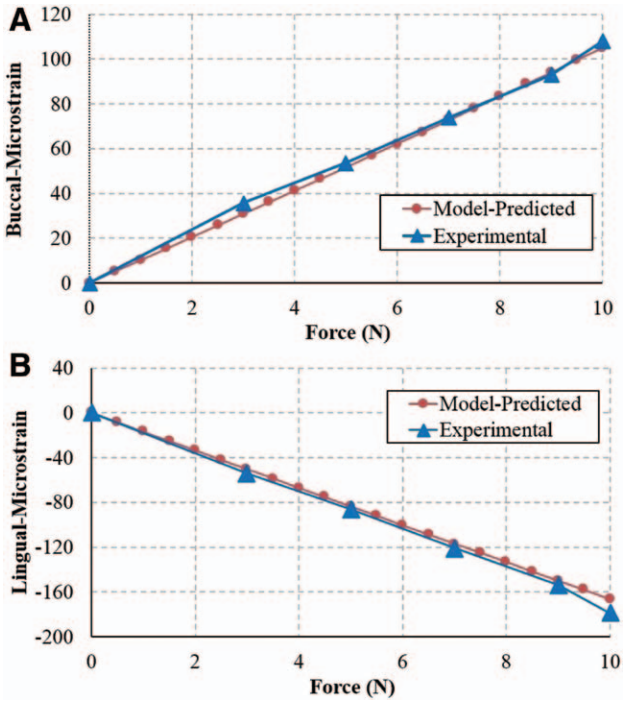

Fig. 1. Model validation: a comparison between experimental data with FE model data in the buccal region placement of the strain gauges (A) and the lingual region (B). The simulations are done using FE.

Stress Shielding of Some of the Grafted Bone and Host Mandible

As shown in Figure 3, stress shielding is reduced in the double-barrel fibular graft as opposed to the single-barrel fibular graft condition. This may be due to the increased continuity between the grafted bone and the host mandible. The highest stress shielding occurs in the anterior regions of the single-barrel fibular graft.

To better understand the stress shielding of the reconstructed mandible, we compared average von Mises stress on the different anatomical regions of the 3 aforementioned cases (Fig. 4). It is shown that stress shielding occurs in both cases of reconstruction most likely because of the very stiff Ti–6Al–4V hardware. Meanwhile, the average von Mises stress is less on the symphysis and alveolar process regions, and more on the body, angle, ramus, condylar process, and coronoid process regions when a single-barrel fibular graft is used. These differences may be due to the reduced height of the bone that is responsible for load-bearing (Fig. 4).

Stress Concentration at Fixation Plates and Screws

As shown in Figures 3B, C, the highest stress concentration occurs on the inferior fixation hardware in the case where a single-barrel fibular graft is used and the stress is 1.57 times that seen in the double-barrel fibular graft simulation. It should be noted that the highest stress concentrations on the superior distal and superior mesial fixation hardware in the case of using double-barrel graft are 54.32 and 67.77 MPa, respectively. In addition, the stress concentration on the screws, which is a common reason for screw pullout and implant failure, was reduced by a factor of 0.69 in the double-barrel reconstruction over that of a single-barrel fibular reconstruction.

Effect of Thickness of the Fixation Plates on the Reconstruction Surgery

Two sets of fixation plates with different thicknesses are considered to study the effect of various thicknesses on stress shielding effect. As depicted in Figure 5, the double-barrel graft with the thicker fixation plates shows decreased stress for the inferior, superior distal, superior mesial fixation plate, and double-barrel fibular graft by the factors of 0.87, 0.91, 0.98, and 0.91, respectively. Similarly, in the case of using the single-barrel graft, the maximum von Mises stress is reduced by the factors of 0.61 and 0.58 for inferior fixation plate and single fibular graft, respectively.

DISCUSSION

Segmental mandibular defects commonly occur after treatment for benign tumors or malignant primary bone neoplasms, or during reconstructive surgery for trauma, infection, senescence, or osteoradionecrosis. Mandibular reconstruction surgery is undertaken to repair the defect and restore and insure the mandible's contribution to chewing, speaking, swallowing, and breathing functions as well as aesthetic form. Current methods for mandibular reconstruction almost uniformly use Ti–6Al–4V fixation hardware and vascularized fibular bone transplantation of either double- or single-barrel fibular grafts. One of the

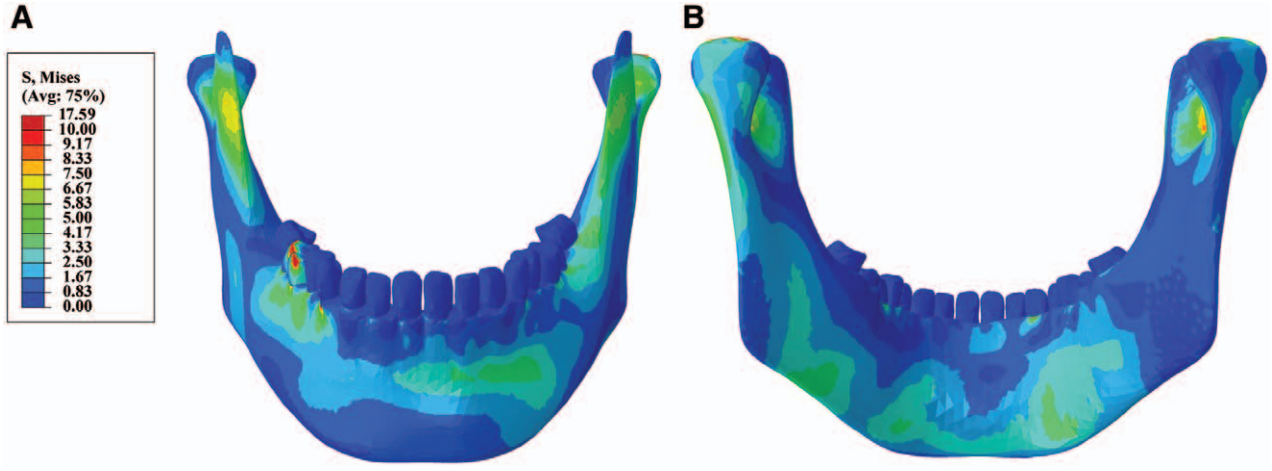

Fig. 2. von Mises stress distribution in a normal mandible during mastication at the right M_1. A, Buccal view. B, Lingual view.

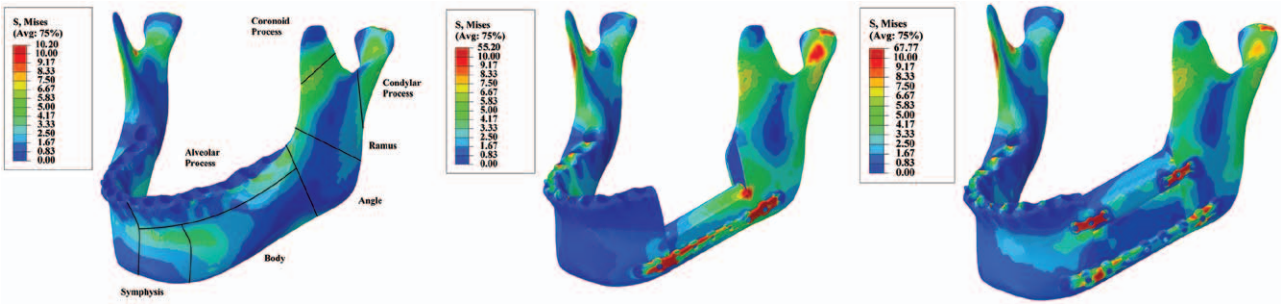

Fig. 3. von Mises stress distribution patterns around the implanted fibular graft during mastication. A, Normal mandible. B, Mandible reconstructed using Ti–6Al–4V hardware and a single-barrel fibular graft. C, Mandibular reconstruction using Ti–6Al–4V hardware and a double-barrel fibular graft (unit: megapascal).

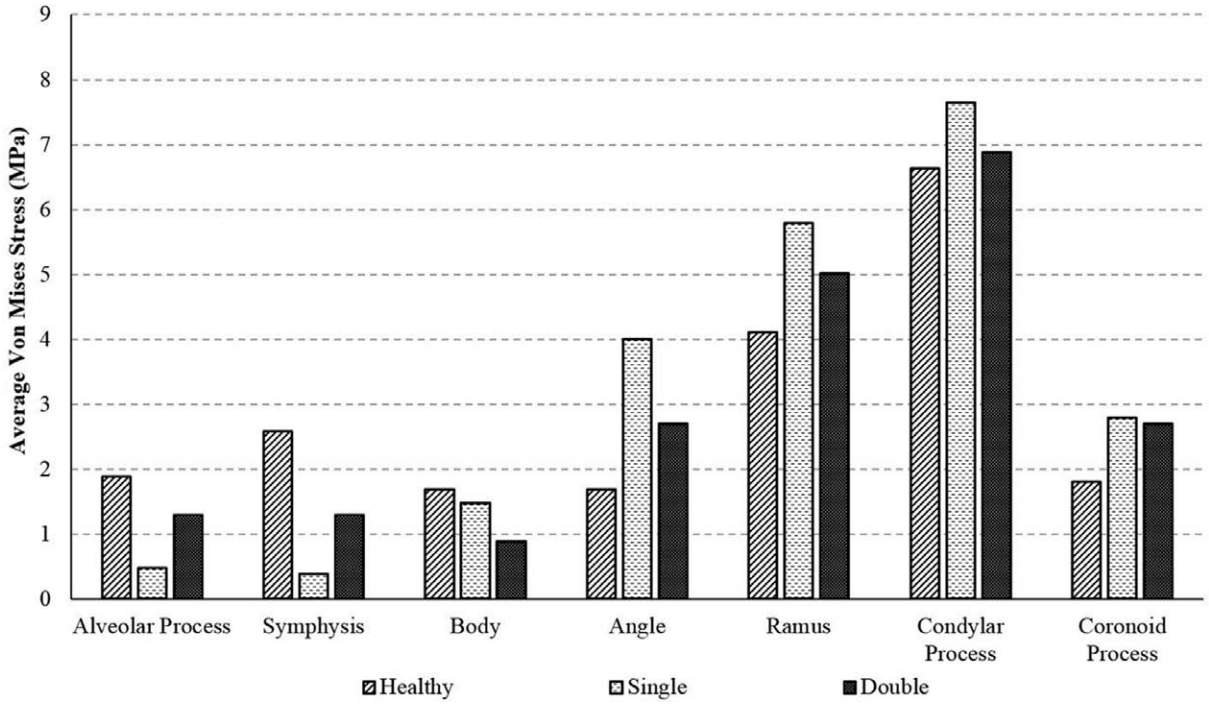

Fig. 4. Average von Mises Stress at 6 different anatomic and functional zones for the following cases: Case I: Reconstructed mandible with a single-barrel fibular graft and Ti–6Al–4V fixation hardware; Case II: Reconstructed mandible with a double-barrel fibular graft and Ti–6Al–4V fixation hardware; and Case III: Normal healthy mandible.

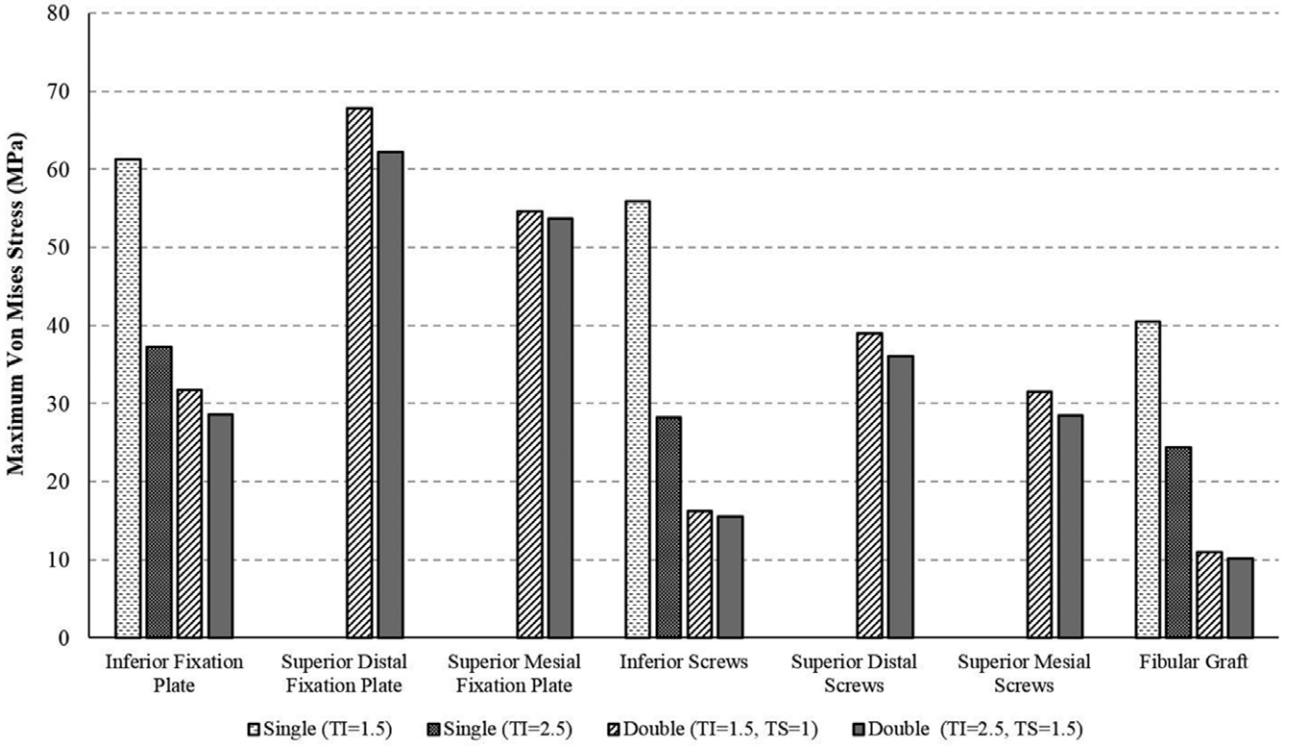

Fig. 5. The comparison of the highest von Mises stress on the model components using 2 different sets of fixation plates with various thicknesses. TI denotes thickness of the inferior plate; TS, thickness of both superior mesial and distal plates.

main challenges in using permanent Ti–6Al–4V fixation plates and screws is the stress shielding and stress concentration caused by the high stiffness of this hardware. Although these biocompatible and very stiff plates provide fixation during healing, it should be noted that the healed bone is thereafter significantly stress-shielded.

We have established a comprehensive FE model to simulate maximal right molar bite force on a normal mandible and the 2 cases of mandibular reconstruction using single- or double-barrel fibular grafts. Our results show that stress shielding occurs in both cases of mandibular reconstruction; however, a more normal stress–strain distribution occurs along the mandible when a double-barrel graft is used. Additionally, a double-barrel graft will be more likely to maintain the normal facial contour of the patient and to support dental implant placement. Finally, the use of thinner fixation plates is more promising because they provide increased stress on the fibular graft after the healing period ends. It should be pointed out that we previously had shown that the use of the thinner plate set (ie, the inferior thickness of 1.5 mm and superior thickness of 1 mm) also supports the healing period by providing enough immobilization.[43] In the future, this type of analysis could incorporate patient-specific information and possibly guide the fabrication and placement of fixation hardware as well as the preparation and placement of bone grafts.

Long-term stress concentration at highly stiff fixation plates and especially metallic screws may put them at risk for fracture or loosening in the future. We observed that a double-barrel fibular graft caused less stress concentration on both the fixation plates and the fixation screws.

CONCLUSION

If fixation hardware is to be implanted permanently for the reconstruction of mandibular segmental defects, it may be useful to study how hardware prepared from less stiff materials, such as nitinol[44] or, possibly, porous nitinol,[43, 45–48] might both provide sufficient immobilization during healing and recreate normal stress–strain trajectories during contralateral and/or ipsilateral (ie, after graft/host healing and the effective masticatory use of dental implants placed in the grafted bone) mastication.

David Dean, PhD
Department of Plastic Surgery
The Ohio State University
915 Olentangy River Road, Suite 2140
Columbus, OH 43212
E-mail: David.Dean@osumc.edu

ACKNOWLEDGMENTS

The authors would like to acknowledge the financial support of Ohio Third Frontier Technology Validation and Start-up Fund (TVSF) grant 15-791.

REFERENCES

1. Schmitz JP, Hollinger JO. The critical size defect as an experimental model for craniomandibulofacial nonunions. *Clin Orthop Relat Res* 1986;205:299–308.
2. Abukawa H, Shin M, Williams WB, et al. Reconstruction of mandibular defects with autologous tissue-engineered bone. *J Oral Maxillofac Surg.* 2004;62:601–606.

3. Schrag C, Chang YM, Tsai CY, et al. Complete rehabilitation of the mandible following segmental resection. *J Surg Oncol.* 2006;94:538–545.
4. Moghaddam NS, Ahmadi MT, Rahmani M, et al. Monolayer graphene nanoribbon p-n junction. Presented at: 2011 IEEE Regional Symposium on Micro and Nanoelectronics (RSM). Kota Kinabalu, Sabah, Malaysia; September 28–30, 2011.
5. Dinh P, Hutchinson BK, Zalavras C, et al. Reconstruction of osteomyelitis defects. *Semin Plast Surg.* 2009;23:108–118.
6. Veiga C, Davim J, Loureiro A. Properties and applications of titanium alloys: a brief review. *Rev Adv Mater Sci.* 2012;32:133–148.
7. Esfahani SN, Andani MT, Shayesteh N, et al. Independent tuning of stiffness and toughness of additively manufactured titanium-polymer composites: simulation, fabrication, and experimental studies. *J Mater Process Tech.* 2016;238:22–29.
8. Moghaddam NS, Elahinia M, Miller M, et al. Enhancement of bone implants by substituting nitinol for titanium (TI–6AL–4V): a modeling comparison. Presented at: ASME 2014 Conference on Smart Materials, Adaptive Structures and Intelligent Systems, Newport, RI; September 8-10, 2014.
9. Moghaddam NS. *Toward Patient Specific Long Lasting Metallic Implants for Mandibular Segmental Defects.* [dissertation]. Toledo, OH: University of Toledo; 2015.
10. Hadi A, Qasemi M, Elahinia M, et al. Modeling and experiment of a flexible module actuated by shape memory alloy wire. Presented at: ASME 2014 Conference on Smart Materials, Adaptive Structures and Intelligent Systems. Newport, Rhode Island; September 8–10, 2014.
11. Moghaddam NS, Jahadakbar A, Elahinia M, et al. The effect of adding dental implants to the reconstructed mandible comparing the effect of using Ti–6Al–4V and Niti hardware. Presented at: Tissue Engineering Part A. New Rochelle, NY; August 2015.
12. Elahinia M, Moghaddam NS, Andani MT, et al. Site-specific material properties and the additive manufacturing of nitinol musculoskeletal implants. Presented at: Tissue Engineering Part A. New Rochelle, NY; August 2015.
13. Rahmanian R, Moghaddam NS, Haberland C, et al. Load bearing and stiffness tailored niti implants produced by additive manufacturing: a simulation study. Presented at: SPIE Smart Structures and Materials+ Nondestructive Evaluation and Health Monitoring. San Diego, California; March 9–13, 2014.
14. Kunchur MN, Dean C, Liang M, et al. Depairing current density of Nd 2− x Ce x CuO 4− δ superconducting films. *Physica C: Superconductivity.* 2013;495:66–68.
15. Rahmani M, Ahmadi MT, Shayesteh N, et al. Current-voltage modeling of bilayer graphene nanoribbon Schottky diode. In: 2011 IEEE Regional Symposium on Micro and Nanoelectronics (RSM). Kota Kinabalu, Sabah, Malaysia; September 28–30, 2011.
16. Bähr W, Stoll P, Wächter R. Use of the "double barrel" free vascularized fibula in mandibular reconstruction. *J Oral Maxillofac Surg.* 1998;56:38–44.
17. He Y, Zhang ZY, Zhu HG, et al. Double-barrel fibula vascularized free flap with dental rehabilitation for mandibular reconstruction. *J Oral Maxillofac Surg.* 2011;69:2663–2669.
18. Lee JH, Kim MJ, Choi WS, et al. Concomitant reconstruction of mandibular basal and alveolar bone with a free fibular flap. *Int J Oral Maxillofac Surg.* 2004;33:150–156.
19. Bidabadi M, Natanzi AHA, Mostafavi SA. Thermophoresis effect on volatile particle concentration in micro-organic dust flame. *Powder Technol.* 2012;217:69–76.
20. Kunchur M, Dean C, Moghadam NS, et al. Current-induced depairing in the Bi 2 Te 3/FeTe interfacial superconductor. *Physical Rev B.* 2015;92:094502.
21. Ahmadi K, Zanjani MM. A new method for image security and data hiding in image. *Am J Sci Res.* 2011;41–49.
22. Lovald ST, Wagner JD, Baack B. Biomechanical optimization of bone plates used in rigid fixation of mandibular fractures. *J Oral Maxillofac Surg.* 2009;67:973–985.
23. Bidabadi M, Dizaji HB, Dizaji FF, et al. A parametric study of lycopodium dust flame. *J Eng Math.* 2015;92:147–165.
24. Raad B, Moghaddam NS, Elahinia M. A numerical simulation of the effect of using porous superelastic Nitinol and stiff Titanium fixation hardware on the bone remodeling. In: SPIE Smart Structures and Materials+ Nondestructive Evaluation and Health Monitoring. 2016.
25. Melton K, Mercier O. The mechanical properties of NiTi-based shape memory alloys. *Acta Metall.* 1981;29:393–398.
26. Rahmani M, Ahmadi M, Webb J, et al. Trilayer graphene nanoribbon carrier statistics in degenerate and non degenerate limits. Presented at: Proceedings of the Sixth Global Conference on Power Control and Optimization. Las Vegas, NV; August 6–8, 2012.
27. Moghaddam N, Ahmadi M, Webb J, et al. Modeling of graphene nano-ribbon Schottky diodes in the parabolic band structure limit. Presented at: Proceedings of the Sixth Global Conference on Power Control and Optimization. Las Vegas, NV; August 6–8, 2012.
28. Bores AP, Schmidt RJ. *Advanced Mechanics of Materials.* 6th ed. New York, NY: John Wiley & Sons, Inc.; 2003.
29. Korioth TW, Romilly DP, Hannam AG. Three-dimensional finite element stress analysis of the dentate human mandible. *Am J Phys Anthropol.* 1992;88:69–96.
30. Fitton LC, Shi JF, Fagan MJ, et al. Masticatory loadings and cranial deformation in Macaca fascicularis: a finite element analysis sensitivity study. *J Anat.* 2012;221:55–68.
31. Ahmadi K, Javaid AY, Salari E. An efficient compression scheme based on adaptive thresholding in wavelet domain using particle swarm optimization. *Image Commun.* 2015;32:33–39.
32. Ahmadi K, Salari E. Small dim object tracking using a multi objective particle swarm optimisation technique. *Image Processing, IET.* 2015;9:820–826.
33. Tadano S, Okoshi T. Residual stress in bone structure and tissue of rabbit's tibiofibula. *Biomed Mater Eng.* 2006;16:11–21.
34. ABAQUS/Explicit: User's Manual. Vol. 1. Providence, RI: Hibbitt, Karlsson and Sorenson Inc.; 2001.
35. Hughes TJ. *The Finite Element Method: Linear Static and Dynamic Finite Element Analysis.* Kendallville, IN: Courier Corporation; 2012.
36. Andani MT, Moghaddam NS, Haberland C, et al. Metals for bone implants. Part 1. Powder metallurgy and implant rendering. *Acta Biomater.* 2014;10:4058–4070.
37. Shetty PP, Meshramkar R, Patil KN, et al. A finite element analysis for a comparative evaluation of stress with two commonly used esthetic posts. *Eur J Dent.* 2013;7:419–422.
38. Nagasao T, Miyamoto J, Kawana H. Biomechanical evaluation of implant placement in the reconstructed mandible. *Int J Oral Maxillofac Implants.* 2009;24:999–1005.
39. Van Eijden TM, Korfage JA, Brugman P. Architecture of the human jaw-closing and jaw-opening muscles. *Anat Rec.* 1997;248:464–474.
40. Ichim I, Kieser JA, Swain MV. Functional significance of strain distribution in the human mandible under masticatory load: numerical predictions. *Arch Oral Biol.* 2007;52:465–473.
41. Bathe K-J. On reliable finite element methods for extreme loading conditions. In: Ibrahimbegovic A, Kozar I, eds. *Extreme Man-Made and Natural Hazards in Dynamics of Structures.* Englewood Cliffs, NJ: Springer; 2007:71–102.
42. Keyak JH. Improved prediction of proximal femoral fracture load using nonlinear finite element models. *Med Eng Phys.* 2001;23:165–173.
43. Moghaddam NS, Skorachi R, Miller M, et al. Three dimensional printing of stiffness-tuned, nitinol skeletal fixation hardware

with an example of mandibular segmental defect repair. *Procedia CIRP*. 2015;6:45–50.
44. Elahinia M, Shayesteh Moghaddam N, Taheri Andani M, et al. Fabrication of NiTi through Additive Manufacturing: A Review. *Prog Mater Sci*. In press.
45. Elahinia M, Moghaddam NS, Andani MT, et al. Mitigating implant failure through design and manufacturing of nitinol fixation hardware. Presented at: Tissue Engineering Part A. New Rochelle, NY; August 2015.
46. Mahtabi MJ, Shamsaei N, Mitchell MR. Fatigue of nitinol: the state-of-the-art and ongoing challenges. *J Mech Behav Biomed Mater*. 2015;50:228–254.
47. Mahtabi MJ, Shamsaei N. Multiaxial fatigue modeling for nitinol shape memory alloys under in-phase loading. *J Mech Behav Biomed Mater*. 2015;55:236–249. *Pattern Recognit*.
48. Ahmadi K, Salari E. Small dim object tracking using frequency and spatial domain information. *Pattern Recognit*. 2016;58:227–234.

APPENDIX

Ti–6Al–4V (surgical grade 5 titanium or Ti64): Ti–6Al–4V is the most common titanium alloy used in medical devices (ie, more than 50% of Ti usage in medical devices). It refers to an alloy made up of 90% titanium, 6% aluminum, and 4% vanadium. This alloy is significantly stronger than pure titanium, yet has a similar stiffness. This material is almost uniformly used in standard-of-care mandibular fixation devices.[6,7]

Finite element model (FE model): The purpose of creating these models is to simulate the real geometry of the structure in a virtual environment. An FE model is a mathematical model, which includes a computer-readable shape of an object of study. Often that shape is represented in the computer as a surface filled with a tetrahedral mesh. The material properties found at each location in the shape are assigned to the nodes of that mesh. The response to loading of the model, such as the loading of bone and bone fixation during chewing, can be simulated by an FE model on a computer. Similarly, solutions for potential problems can be simulated and then tested in the laboratory (in vitro) or in an animal model (in vivo), cadaver, or, once justified, in a patient.[35]

Finite element analysis (FEA): FEA is a numerical analysis that evaluates deformation, stress, and strain that occur within the structures observed in response to physical effects such as internal/external forces or vibrations that can be simulated by an FE model. For example, an FEA is the portion of this mathematical analysis, which calculates the effect of a particular load on the FE model. As with the model, an FEA calculation divides the entire model's geometry into a series of subdivisions, namely elements, with simpler geometry but similar properties to make the calculation tractable.[35]

ABAQUS: ABAQUS (Dassault Systèmes, Waltham, Mass.) is one of the most common FE model/FEA software programs.[34]

Mesh: Creating a mesh to fill a solid object allows division of the overall calculation needed for an FEA into a series of smaller subregional problems within the overall 3D FE model. It is crucial to assign an appropriate, proper size and distribution to the mesh elements. Doing so ensures the independence of the results from the mesh sizes.[34]

Material properties: Material properties (eg, modulus of elasticity) explain the response of the material to the physical effects such as internal/external forces. A qualitative measure of material properties is used to identify and classify materials.[25]

Modulus of elasticity, E (Young's modulus, elastic modulus, or stiffness): It is the slope of the linear region of the stress–strain curve attributes to a material. (The unit is Pascal [Pa].)[25]

Modulus of rigidity, G (shear modulus): It is the slope of the shear stress–strain curve attributed to a material. (The unit is Pascal [Pa].)[25]

Poisson's ratio, v: It is the transverse contraction strain in response to longitudinal extension. It is a dimensionless quantity.[25]

Reaction force: Reaction force is a force that is acting in the opposite direction. In the case of teeth, the summation of the reaction forces between the bite contact is equal to bite force.[29,30]

Strain: It is a relative deformation of 2 different points along the structure.[28]

Stress: Stress is a physical quantity that describes the internal forces created within the structure to balance external forces.[28]

Von Mises stress: von Mises stress is a non-negative scalar measurement of the stress on the structure. The maximum von Mises stress failure criterion is often used by engineers to evaluate whether the structure (eg, the mandible) undergoes failure under normal loading. On the basis of this theory, the material will yield when the maximum von Mises stress reaches its stress limit (eg, the yield strength).[42]

Residual stress: When the original cause of stress formation is removed, a small portion of the imposed stress may remain, which is called residual stress. Residual stresses are often caused because of plastic deformations, temperature gradients, and structural changes.[33]

The factor of safety (FoS): It is often known as the ratio of ultimate stress to the calculated maximum stress when the structure is in use.[33]

X, y, and z vectors: In this study, the vector direction (right–left) is normal to the sagittal plane, with the positive direction pointing toward the left side of the mandible. The vector direction (superior–inferior) is normal to the occlusal plane, with the positive direction pointing superiorly. The vector direction (anterior–posterior) is orthogonal to the remaining 2 orthogonal axes.

***Zx*, *zy*, and *xz* planes:** The *zx* and *zy* planes correspond to the occlusal plane and the sagittal plane, respectively. The *xz* plane describes the plane perpendicular to these 2 planes.